ANL/CP--74487

DE92 014764

THE IMPACT OF DUCT-TO-DUCT INTERACTION ON THE HEX DUCT DILATION*

By

M. J. Lee, L. K. Chang, C. E. Lahm and D. L. Porter
Argonne National Laboratory
9700 South Cass Avenue
Argonne, Illinois

To be presented at the
1992 ASME PVP Conference
New Orleans, Louisiana
June 21-25, 1992

*Work supported by the U. S. Department of Energy, Nuclear Energy Programs under Contract No. W-31-109-ENG-38

THE IMPACT OF DUCT-TO-DUCT INTERACTION ON THE HEX DUCT DILATION*

M. J. Lee, L. K. Chang, C. E. Lahm and D. L. Porter
Argonne National Laboratory
Argonne, Illinois

ABSTRACT

Dilation of the hex duct is an important factor in the operational lifetime of fuel subassemblies in liquid metal fast reactors. It is caused primarily by the irradiation-enhanced creep and void swelling of the hex duct material. Excessive dilation may jeopardize subassembly removal from the core or cause a subassembly storage problem where the grid size of the storage basket is limited. Dilation of the hex duct in Experimental Breeder Reactor II (EBR-II) limits useful lifetime because of these storage basket limitations. It is, therefore, important to understand the hex duct dilation behavior to guide the design and in-core management of fuel subassemblies in a way that excessive duct deformation can be avoided.

To investigate the dilation phenomena, finite-element models of the hex duct have been developed. The inelastic analyses were performed using the structural analysis code, ANSYS. Both Type 316 and D9 austenitic stainless steel ducts are considered. The calculated dilations are in good agreement with profilometry measurements made after irradiation. The analysis indicates that subassembly interaction is an important parameter in addition to neutron fluence and temperature in determining hex duct dilation.

INTRODUCTION

Permanent deformation of austenitic 316 SS ducts is caused primarily by irradiation-enhanced creep and void swelling. Excessive dilation may jeopardize subassembly removal and delay reactor startup. Both the Fast Flux Test Facility (FFTF) and EBR-II have experienced this problem in their operation history as reported by Makenas (1990) and Seidel (1986). In addition, the EBR-II has had further difficulty to place the overly dilated subassembly in the storage basket, which can only accommodate a limited dilation of 1.016 mm (40 mils). This problem has caused the EBR-II to restrict the irradiation of its driver subassemblies to a maximum 10 at.% burnup, which is equivalent to a high energy ($E \geq 0.1$ MeV) fluence exposure of 1.0×10^{23} n/cm^2.

To extend the burnup limits of the subassembly the titanium-stabilized austenitic D9 claddings and ducts have been extensively tested in the United States. The D9 material is known for its high incubation fluence threshold for the onset of the volumetric swelling (Washburn, 1986), which can significantly delay the swelling part of dilation until high burnup. The FFTF in-pile test results have indicated that the D9 material can reduce the peak duct dilation to as much as one third of what is expected from 316 SS under the same irradiation condition (Makenas, 1986). Thus, the benefit of using D9 duct for dilation reduction was demonstrated and the swelling resistance of D9 was accredited.

The irradiation of D9 ducts and fuel cladding in EBR-II has been conducted under the Integral Fast Reactor (IFR) program at Argonne National Laboratory (ANL). Many subassemblies have been irradiated and the benefit of using D9 was confirmed until difficulties were encountered with test subassembly X435. This subassembly belonged to a group of four D9 subassemblies designed to be irradiated continuously without reconstitution to high burnup. While the other three subassemblies were blanket drivers positioned in reactor outer row six, X435 was a typical core-type driver irradiated in reactor inner row two. At the end of irradiation the X435 ducts had accumulated a fluence of 14.7×10^{22} n/cm^2 and incurred a peak flat-to-flat dilation of 2.03 mm (80 mils), which was twice the original design limit. The large dilation was unexpected for two reasons: first, if the major mechanism behind duct dilation was volumetric swelling, a simple calculation from post-irradiation profilometry would indicate an apparent volumetric swelling of 10.5%, which would be too high to match what the U.S. D9 database would predict at a temperature of 420°C; secondly, a later immersion density measurement on the duct material showed a volumetric swelling not more than 1%, which confirmed the low swelling of D9 and indicated that creep may be the real cause for the large dimensional change. This incident demonstrated a complicated dilation phenomenon, which may not be solved simply by employing an alloy having low swelling capability such as D9 material.

To understand the duct dilation phenomenon and to delineate the associated process in the reactor, a mechanistic analysis of the in-pile duct behavior was conducted taking advantage of the database of D9 creep and swelling properties obtained through many experiments. In the analysis finite element models (FEM) of the driver subassembly in EBR-II were developed to interpret the profilometry data meaningfully and to elucidate the roles of creep and swelling in duct dilation. This paper describes the duct configuration and its reactor environment, continues with the FEMs of in-reactor behavior, and concludes with a discussion of the dilation process and its implication on reactor operation.

HEX DUCT DESCRIPTION

The typical driver subassembly in the EBR-II reactor is shown in Fig. 1. It consists of a hex duct with a top-end fixture and a lower-end adapter; a total of 61 fuel pins arranged concentrically in five rows are housed within. The hex duct is 1.676 m (66 in.) long and is made from either 12% cold-worked 316 SS or 20% cold-worked D9 material. The duct wall is 1.02 mm (0.04 in.) thick and has an inside flat-to-flat dimension of 56.13 mm (2.21 in.). Along the length of the hex duct, 38.1 mm (1.5 in.) above the core midplane, there are six buttons of 0.50 mm (0.02 in.) diameter and 0.36 mm (0.014 in.) high that are cold pressed on six flats. These buttons work together with the bottom nozzle in the grid plate to keep the subassemblies in place and set the clearance between them at the beginning-of-life (BOL). During irradiation the high temperature environment tends to anneal the residual stresses left in the buttons at the time of cold forming. The buttons tend to flatten under creep as tight contact between adjacent subassemblies occurs due to thermal expansion, internal coolant pressure and duct dilation. The fuel pins contain sodium-bonded U-10Zr fuel and have a cold worked 316 SS or D9 cladding of 5.84 mm (0.23 in.) outside diameter and wire wraps of 1.07 mm (0.042 in.) made of the same material; the cladding thickness is 0.38 mm (0.015 in.). There is clearance between the fuel bundle and the inner surface of the hex duct. A preliminary analysis of the subassembly indicates that there will be no interaction between fuel bundle and duct at 10 at.% or lower burnup regardless of whether 316 SS or D9 duct materials are used.

HEX DUCT ENVIRONMENT

In EBR-II the peak fast flux at inner row two is 2.94 x 10^{15} n/cm^2-sec., and it decreases slowly toward the outer row six of the core. It drops rapidly at the inner blanket row seven to slightly less than half of the peak value in row one. Axially the fast flux peaks approximately at the core midplane and the flux at the core bottom is higher than at the top. The peak to average flux ratio is approximately 1.2 over the 34.3 cm (13.5 in.) core. The fast flux has a strong influence on the creep and swelling of the duct. Post-irradiation examination (PIE) of both 316 SS and D9 ducts has clearly indicated that the peak duct dilation always occurs near the core midplane. The thermal-mechanical loading in the duct comes from the coolant flow which generates axial gradients of temperature and pressure. Both gradients are fairly linear in the core region and opposite in direction from bottom to top. The metal temperature of the duct increases from 371°C to ~494°C at reactor row two and to ~533°C at row six. The pressure difference across the duct wall decreases from 289.4 kpa (42.0 psi) at row two and 75.8 kpa (11.0 psi) at row six to virtually zero. Compared with the fuel element plenum pressure, 8.96 Mpa (1300 psi), the net pressure acting on the duct wall appears deceivingly small, yet the flexural stresses it generates, especially at the hexagon corners, are quite significant; it is the influential factor in the creep component of duct dilation. Interactional loading of the duct comes from either duct bowing or dilation, causing the ducts to contact each other and prompting mutual interactions among subassemblies. For the EBR-II driver subassemblies the duct bowing is minor making duct expansion the major cause for the interactional loading. This loading, as we shall see later, is the most intriguing factor in governing hex duct dilation.

HEX DUCT MODEL

Two finite element models were developed to assess the performance of the hex duct during steady state irradiation. The three dimensional (3-D) model, as partly shown in Fig. 2, was first built to simulate the whole hex duct. Plastic quadrilateral shell elements are used to perform elastic and/or plastic analysis. It was intended to study the dilation of the duct which has an asymmetrical circumferential loading and a linear axial loading. The preliminary 3-D analysis, however, showed that the 5% flux tilting and radial temperature gradient across the hex duct caused only a slight deviation in stress and strain from the case of symmetrical loading. The numerous elements in this 3-D model also require a lot of CPU time in many iterations. Furthermore, the large aspect ratio of the duct length over the flat-to-flat distance diminishes significantly the effect of linear axial load. Therefore, the duct dilation was treated as a plain strain problem and a two dimensional (2-D) model, shown in Fig. 3, was subsequently developed.

Because of symmetry of the hex duct geometry and loading, the 2-D model need consist only of one-sixth of the cross section of the duct, extending from the center of one flat to the center of an adjacent flat. Thus, the behavior of the hex duct at a certain elevation may be represented by the 2-D model subjected to the loadings at the same elevation. The model was meshed with one hundred and four nodes. A total of 80 2-D isoparametric solid elements were used to delineate the cross-thickness detail of the flat and corner of the hex duct. The 2-D interface elements were attached to both centers of the flats to model the duct-to-duct interaction. These elements represent two surfaces that may contact, break or slide relative to each other. Their stiffness was taken to be that of the duct at the center of the flat. Boundary conditions at

the centers of the two flats are defined in two mutually perpendicular directions. The displacements along the median planes of the two flats are completely restrained and those in the other direction are set free. Furthermore, the displacements of all nodes in the direction perpendicular to the cross section of the duct are restrained to reflect the plain strain condition. The material properties of the D9 and 316 SS were obtained from Hanford Engineering and Development Laboratory (HEDL). The irradiation-enhanced creep and stress-free swelling correlations were taken from the same source.

ANSYS structural analysis code ("ANSYS Engineering Analysis System," Rev. 4.4) was used for the hex duct analysis. ANSYS is a well accepted structural analysis code that has been widely used to analyze U.S. reactor components. Since the dilation calculation is highly nonlinear, the time step was kept very small to ensure solution convergence. For the case of the 2-D model, a total of 1000 time steps was needed to cover the subassembly irradiation history of 15.0 x 10^{22} n/cm^2 at.% burnup (1.58 x 10^4 hours). The ratio of incremental inelastic strain over elastic strain was kept less than 25% during iteration and the solution was stable and well behaved. A CPU time of 44 minutes on the DEC VAX 8700 was required for the calculation.

RESULTS OF DUCT ANALYSIS

The models were first validated with the analytical close-form solutions to assure the numerical accuracy. Then the pressure and temperature loadings were applied to the 3-D model of the driver subassembly. The resulted stresses and displacements at a specific elevation were compared with those calculated from the 2-D model using the loadings at the same elevation. The maximum discrepancy was within five percent; this was good enough to justify the plain strain assumptions of the 2-D models. In addition, the displacements in the median plan at the center of the flat was found very small which validates the assumed boundary condition. The 2-D model was finally applied to a number of test subassemblies that were made of D9 and 316 SS duct materials and irradiated at grid positions row two and row six, so the dilation simulation would be more representative of the core-wide behavior.

Interaction Among Subassemblies

In the dilation calculations the duct-to-duct interaction among adjacent subassemblies is an important factor needed to be closely examined. To understand the nature of the interaction, the 2-D model was applied to a standard 316 SS driver subassembly irradiated at reactor row two where a fast flux of 2.24 x 10^{15} n/cm^2-sec. was expected. A temperature of 420°C and a coolant pressure difference of 0.1791 MPa (26 psi) was imposed on the duct as the thermal-mechanical loading. The initial clearance between adjacent subassemblies were set at twice the height of the button or 0.712 mm (28 mils). It should be noted that during reactor operation these buttons were thermally annealed early in life and gradually flattened by the contact pressure between subassemblies. Their effect is localized as revealed by duct profilometry and was not considered in the modelling. Through this calculation, which covered an irradiation period of 5.4 x 10^7 sec., the mechanism of the duct-to-duct interaction was better understood. As shown in the stress and strain rate diagram, Fig. 4, the duct flat-to-flat dimension first expands under thermal expansion, pressure-induced duct deformation and irradiation-induced creep up to a fluence of 2.1 x 10^{22} n/cm^2. During this period the stresses in the duct are fairly constant. The cumulated strain is primarily caused by creep and the swelling strain is virtually

zero. Then the creep strain rate ascends quickly until a fluence of 3.0 x 10^{22} n/cm^2 is reached where the contact between adjacent hex ducts starts. The interaction reduces the stresses significantly as the contact area spreads, which causes the creep rate to drop accordingly and reduces further creep contribution. As the creep impact recedes, the swelling component of the dilation is still in the incubation stage until the duct reaches a fluence of 6.0 x 10^{22} n/cm^2. During this period the duct dilation histogram, as shown in Fig. 5, exhibits a plateau, a transition of mechanism in which swelling is about to take over from creep. The duct dilation eventually rises again as the swelling takes control and becomes the major mechanism. Once the swelling-driven dilation begins it is not deterred by the interaction because it is load independent. The duct will continue to expand until the end of irradiation. The total dilation calculated was 0.64 mm (25.3 mils) after the fluence reached 12 x 10^{22} n/cm^2, 1.40 mm (55 mils) less than if the interaction did not take place early and the creep component were not severed. Thus, the timing at which the duct-to-duct interaction begins is crucial in restricting the duct dilation. Consequently, the initial clearances between the subassembly and its neighbors at the beginning of irradiation needs to be carefully managed to give a favorable timing of interaction.

Two Limiting Cases

Core management in EBR-II requires extra effort to accommodate the insertions of numerous experiments. Any subassembly at the time of core loading may face neighbors having quite different irradiation histories, which would result in different initial clearances and subsequent interaction of unique timing and fashion. Thus, there are as many different degrees of duct-to-duct interaction as there are subassemblies and it is impractical to trace each one of them. To account for the variance in the effects of different duct interactions on the dilation, the analyses categorize them into two limiting cases according to the degree of interactions among neighboring ducts. The duct-to-duct interaction usually occurs late in life when the subassembly under consideration has much higher irradiation time/exposure than its neighbors at the inception of irradiation. In this case the hex duct of the subassembly would grow uninhibited at the expense of the slow growing neighbors until the initial gap between them is closed. The early duct-to-duct interaction, on the other hand, occurs when the subassembly considered has either lower than or same irradiation time/exposure as its neighbors. The hex duct growth would be limited by its neighbors through early closing of the gap. Other cases would fall between these two limiting cases. A total of nine test subassemblies were chosen for the investigation and validation of the limiting cases, the detailed discussions of which follow:

1. Late Duct-to-Duct Interaction

   The first data used for this analysis came from the profilometry measurements of the D9 duct of the test subassembly X435. This duct had accumulated a fluence of 14.7 x 10^{22} n/cm^2 (E>0.1 MeV) at EOL after 10 reactor runs (from run 144A through run 153). The irradiation history of X435 indicated that it was positioned at grid location 2D1 for all runs while its six neighbors were replaced after a fluence of 6 x 10^{22} n/cm^2 had been reached. A total of 16 fresh or low exposure subassemblies were irradiated afterwards at the six positions adjacent to X435 until the end of irradiation. The records showed that none of these 16 surrounding subassemblies stayed longer than two reactor runs, which were equivalent to 2.5 to 3.0 x 10^{22} n/cm^2. Consequently, the X435 subassembly was always irradiated

among neighbors that did not have much dilation. This would provide a relatively free expanding environment for the subassembly. The 2-D model simulated this case by setting the initial gap of the interface element to a large value. The temperature and coolant pressure loadings of the duct are 420°C and 0.179 Mpa (26 psi), respectively. When the components of the duct dilation was delineated, the creep contribution of 1.98 mm (78 mils) far outweighed those from void swelling 0.196 mm (7.7 mils). The volumetric swelling of D9 is based on the the data from HEDL. The post-irradiation measurement of the immersion density of X435, however, indicated a volumetric swelling of 0.8%, which translates into a dilation contribution of 0.15 mm (6.0 mils). The resulted maximum flat-to-flat dilation of 2.03 mm (80 mils), Fig. 6 agreed well with the profilometry measurement.

2. Early Duct-to-Duct Interaction

The profilometry measurements on ducts from eight 12% CW 316 SS of EBR-II driver subassemblies were analyzed for this case. These subassemblies were categorized into two groups according to fuel burnup (exposure) and grid positions during irradiation. The first group of three subassemblies, which accumulated a fluence of 8.4 to 10 x 10^{22} n/cm^2, were located in rows two and three. The other group of five subassemblies which accumulated fluences of 6.5 to 8.0 x 10^{22} n/cm^2, were located in rows six and seven. Irradiation histories of the subassemblies revealed that these driver subassemblies have been rotated and repositioned in reactor during their lifetime so that they were kept at a similar burnup as their neighbors. This practice, whether by accident or by design, has made the driver subassembly clusters rather homogeneous in burnup. Therefore, all subassemblies would grow in a similar fashion and interact with each other at early stage of irradiation. Early duct-to-duct interaction, as explained previously, would inhibit the dilation contribution from irradiation-induced creep. As a result, the diametral dilation of these hex ducts may have been influenced at an early stage of irradiation by its adjacent neighbors. The results of the analyses are shown in Fig. 7 and they agree very well with the test data. The 2D-model with the gap elements worked reasonably well. The major assumption made in the calculation was that the gap size between subassemblies was assumed to be twice the depth of hex buttons, 0.711 mm (28 mils). The plateau in the dilation vs. fluence plot indicates the change in mechanism from creep to swelling. It deters the dilation until the swelling component become effective. The swelling contribution is likely to be much less affected by button-to-button contact between subassemblies.

CONCLUSION

The hex duct dilation investigation led us to the following conclusions:

1. The hex duct dilation phenomenon is better understood through mechanistic models, which are able to synthesize the irradiation history, external loading and

constitutive laws of the hex duct to make meaningful interpretation of the underlying mechanism and to predict dilation behavior.

2. The dilation mechanism, as modeled here, can be delineated into two stages:

   - The first stage sees a gradual closing of the inter-subassembly gap by irradiation-induced creep of the hex ducts. The swelling contribution is comparatively small.

   - The second stage starts when the inter-subassembly gap is closed. The duct-to-duct interaction takes the pressure load off the duct wall. The creep-induced dilation abates and the swelling contribution takes over.

3. In view of the potential importance of the duct-to-duct interaction on duct dilation, subassemblies with large differences of burnups should not be placed next to each other. A frequent replacement of fresh subassemblies next to one with high fluence may tend to aggravate the total dilation.

4. To further test the accuracy of the mechanistic model more profilometry data of irradiated 12% CW 316 SS ducts from EBR-II should be analyzed. These ducts should be selected and sorted according to the irradiation histories of their neighbors so that the influence of duct-to-duct interaction on dilation can be further elucidated.

REFERENCES

Makenas, B. J., "Performance of Titanium Stabilized DE Cladding and Ducts," *International Conference on Reliable Fuels for LMR*, pp. 3-52, Sept. 1986.

Makenas, B. J., Chastain, S. A. and Gneiting, B. C., "Dimensional Changes in FFTF Austenitic Cladding and Ducts," *Proceedings, ANS Annual Meeting on LMR: A Decade of LMR Progress and Promise*, Nov. 11-15, 1990.

Seidel, B. R., Porter, D. L., Walters, L. C. and Hofman, G. L., "Experience with EBR-II Driver Fuel," *Proceedings, ANS International Conference on Reliable Fuels for Liquid Metal Reactors*, Sept. 7-11, 1986.

Swanson Analysis Systems, Inc., Houston, PA, "ANSYS Engineering Analysis System," Rev. 4.4.

Washburn, D. F. and Weber, J. W., "FFTF Driver Fuel Experience," HEDL-SA-3468-FP, Westinghouse-Hanford Company, Richland, WA, 1986.

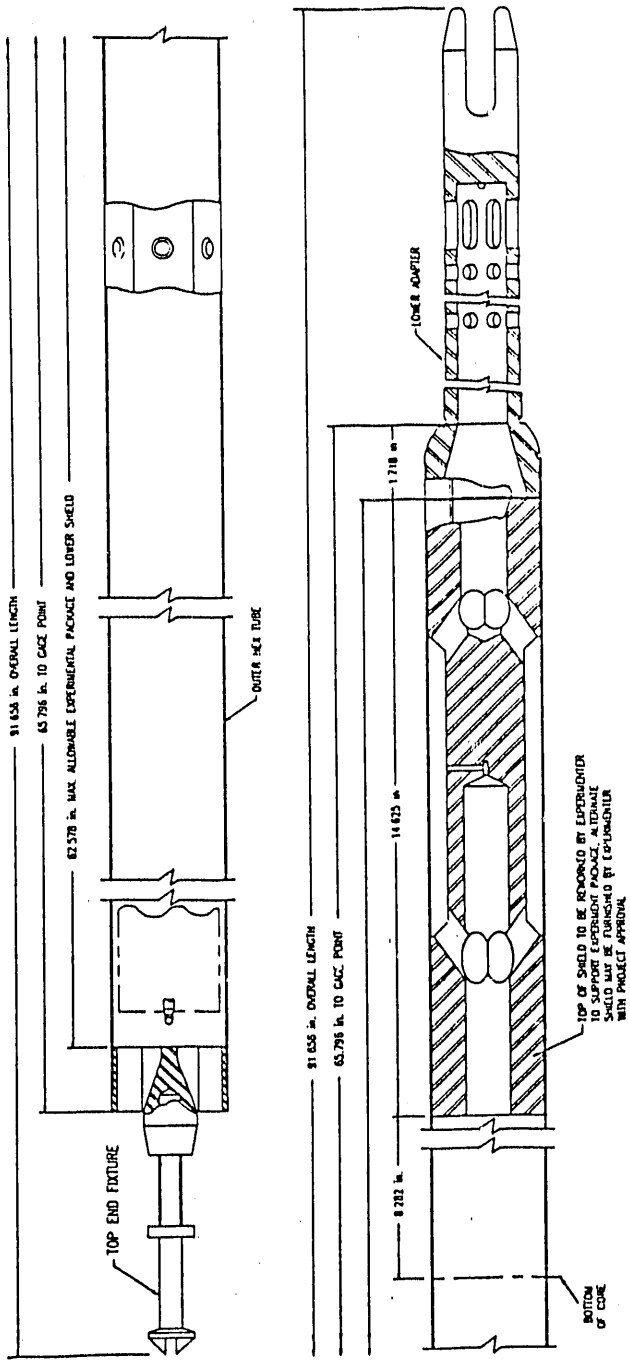

Fig. 1 Typical EBR-II Drive Subassembly

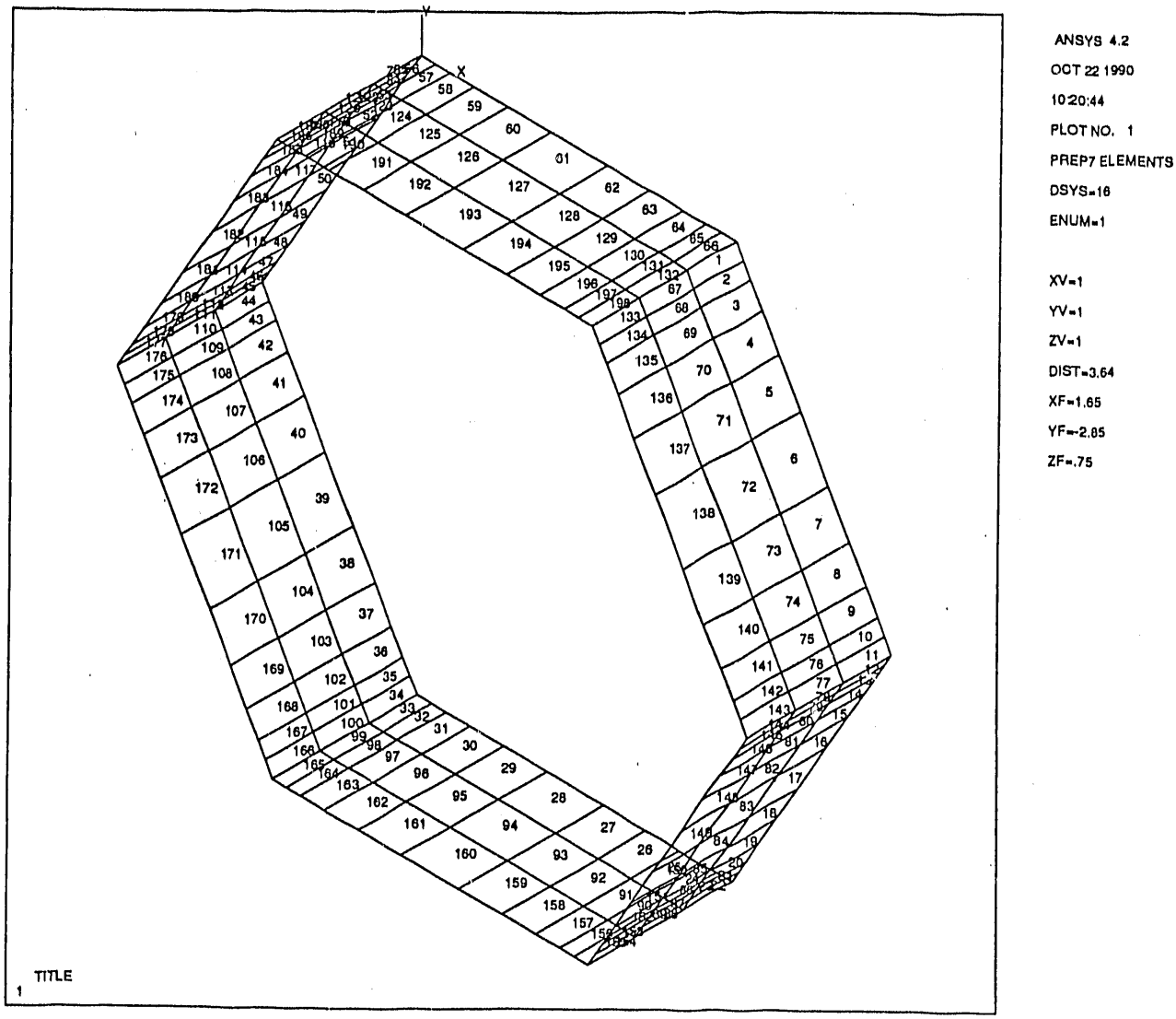

Fig. 2 Partial View of Three-Dimensional Hex Duct Model

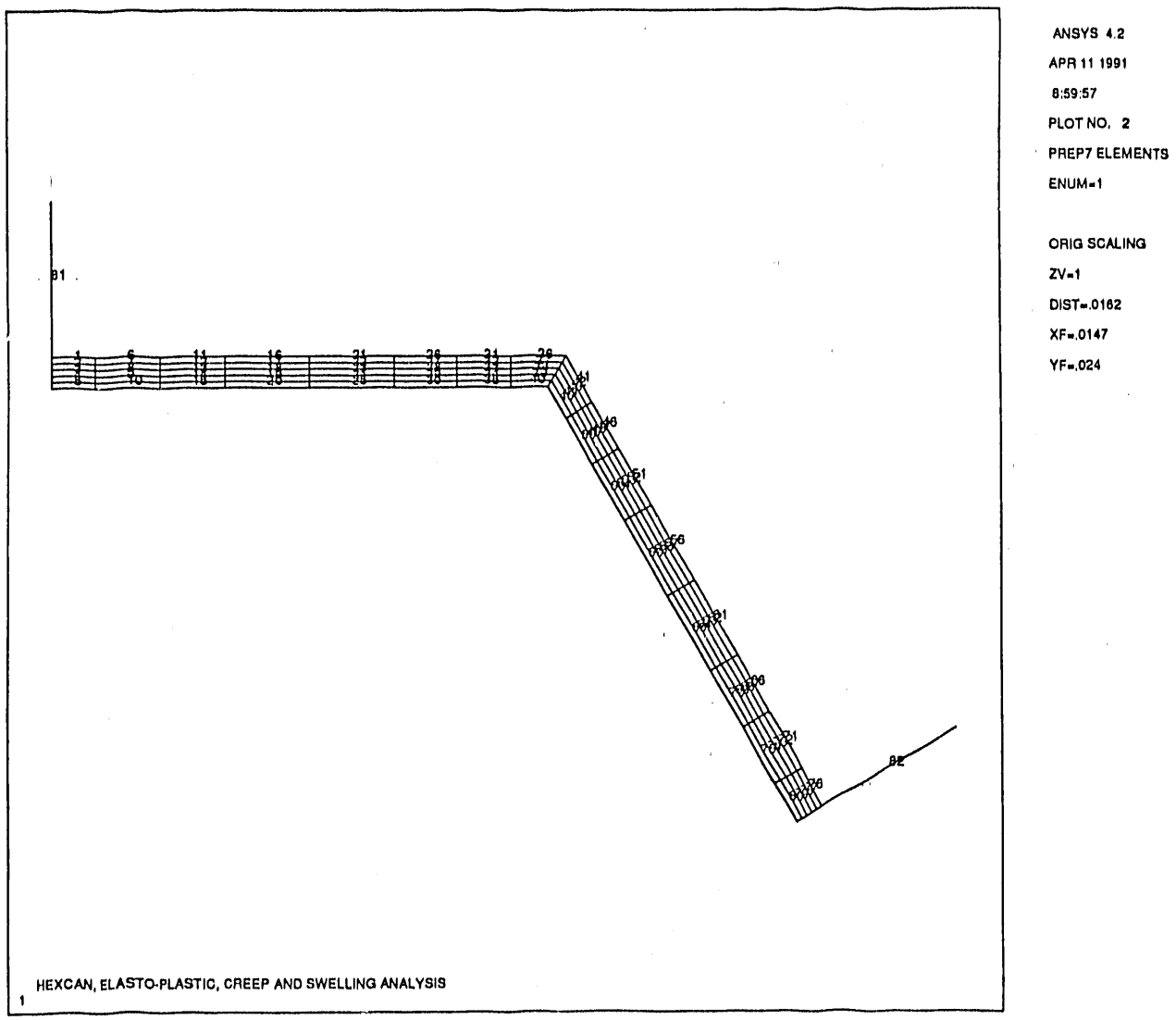

Fig. 3 Two-Dimensional Hex Duct Model

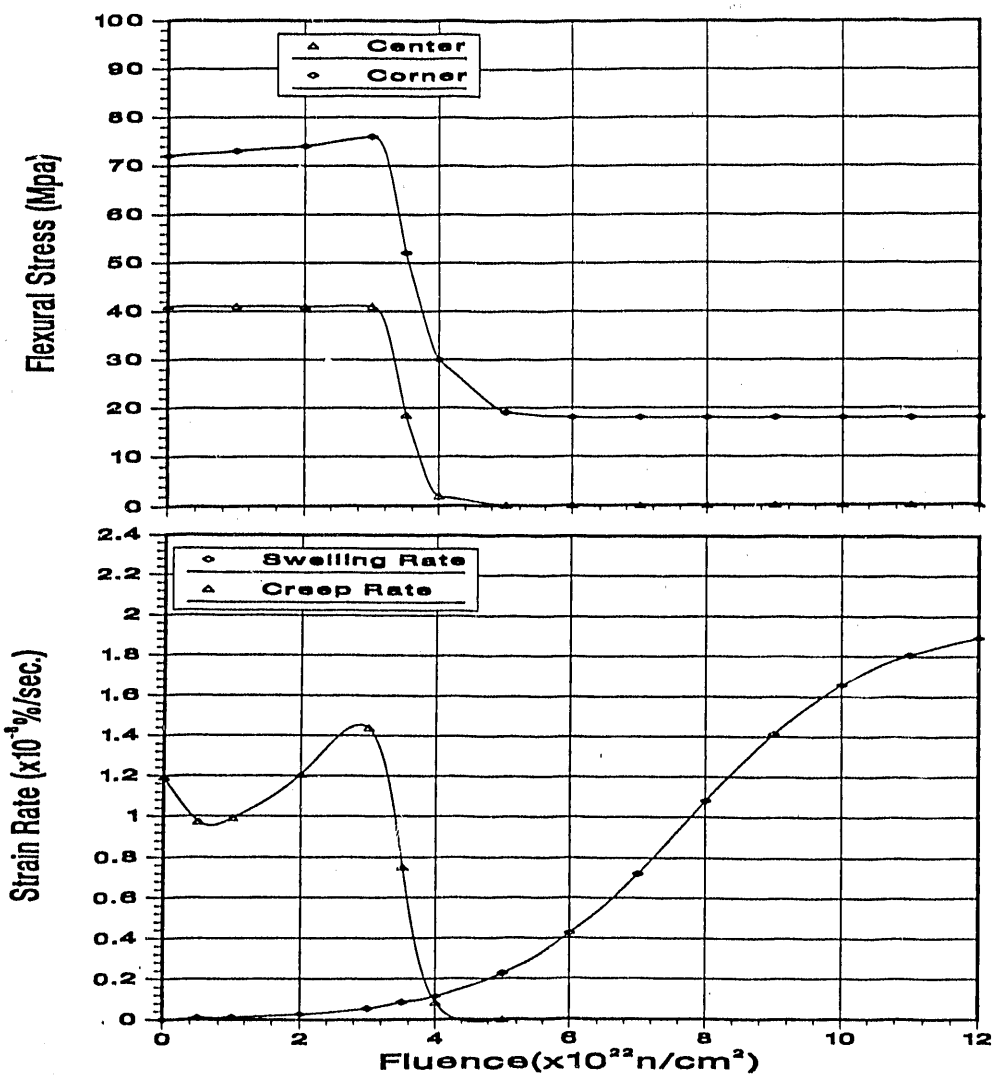

Fig. 4 Stress and Strain Rate Variation During Duct-to-Duct Interaction

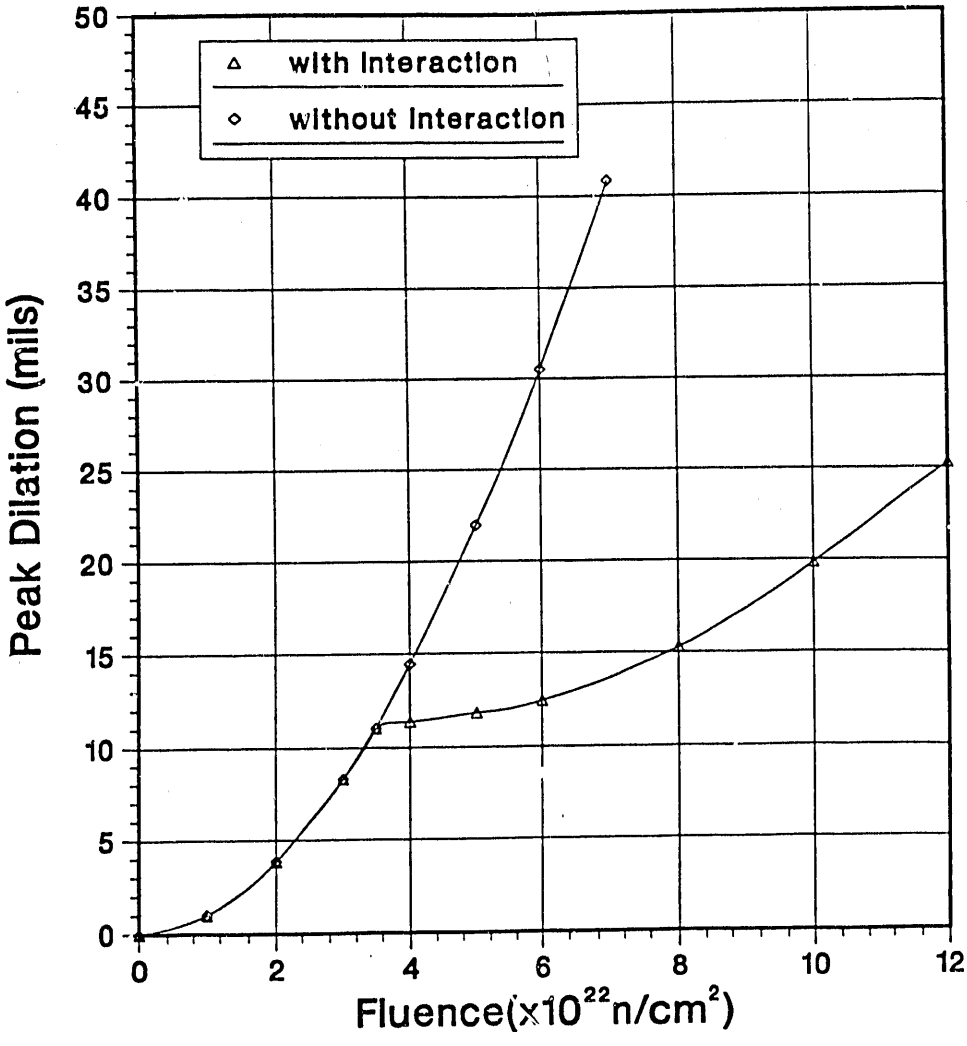

Fig. 5 Variation of Peak Dilation With and Without Interaction

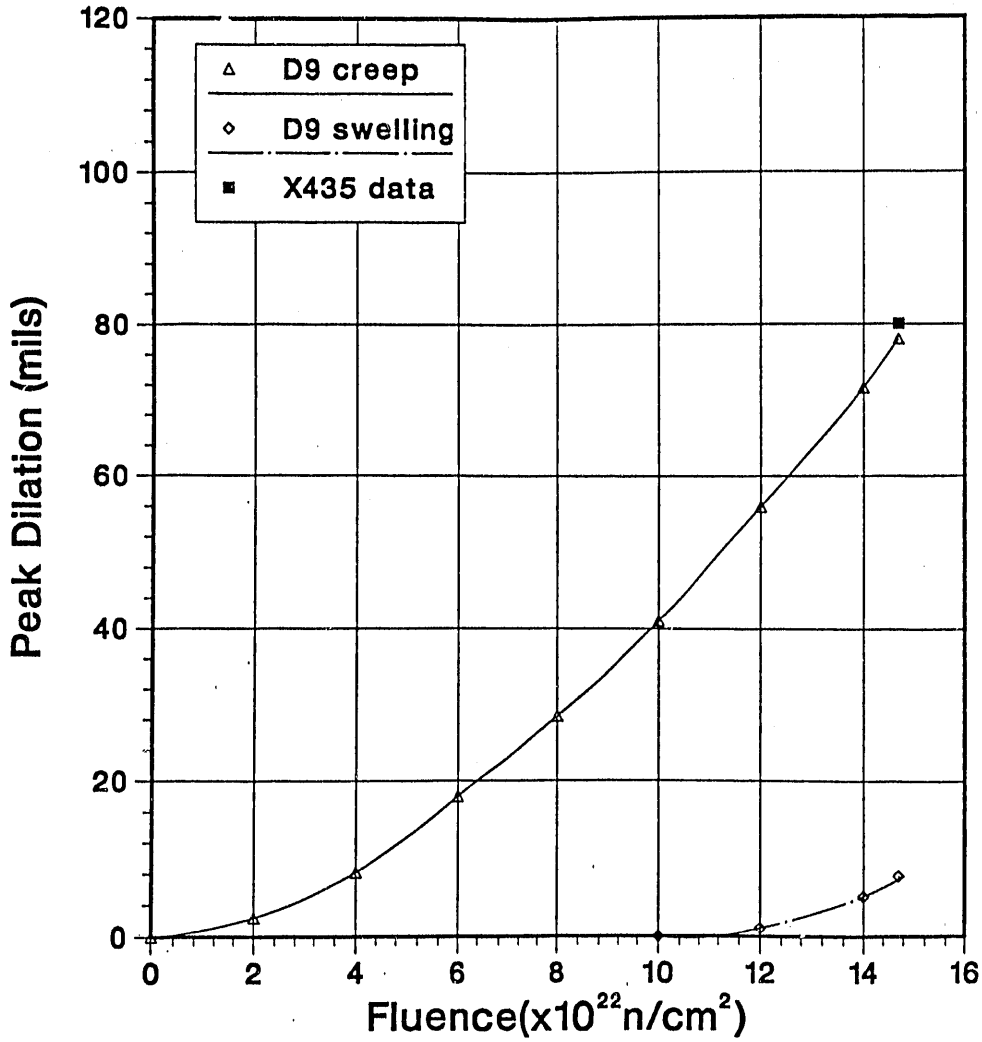

Fig. 6 Comparison Between the Calculated and Measured Peak Dilation of D9 Hex Duct

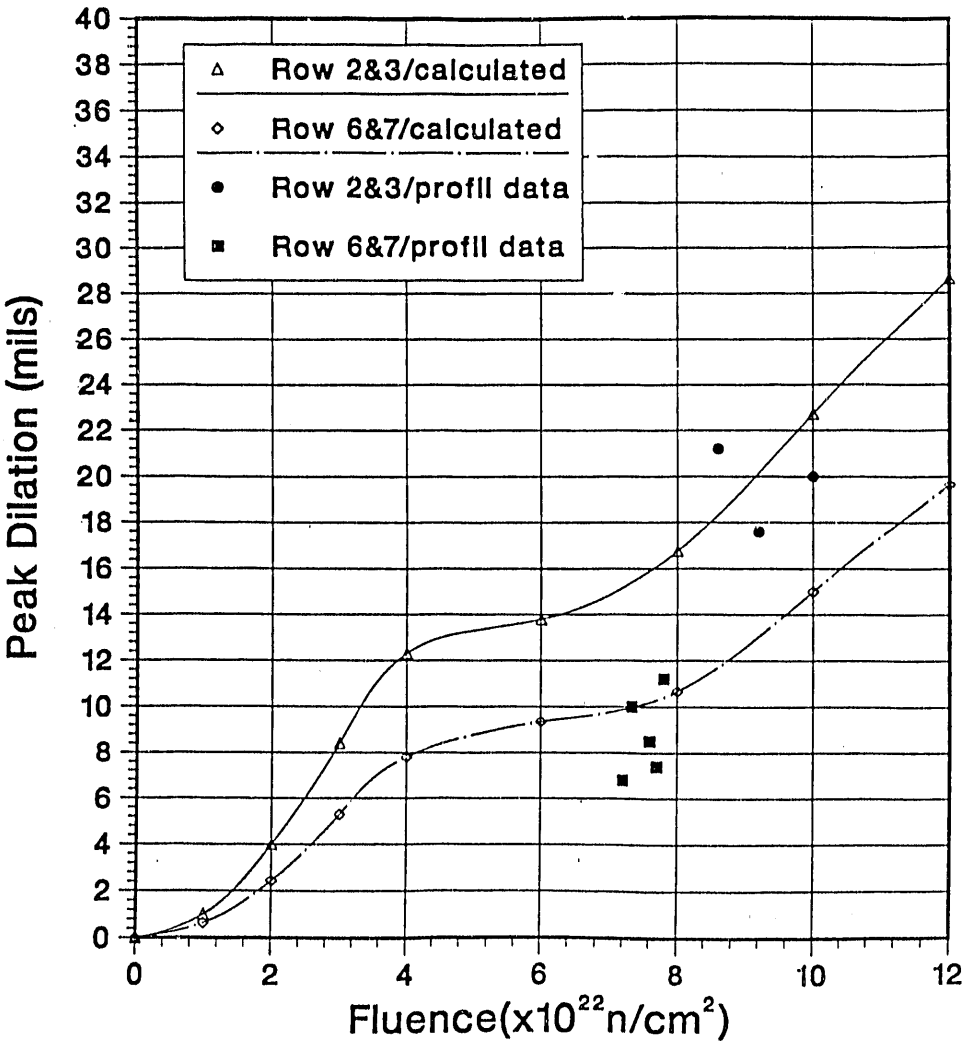

Fig. 7 Comparison Between the Calculated and Measured Peak Dilation of SS316 Hex Duct

DATE
FILMED
7/7/92